Bioorganic Chemistry 113 (2021) 104994

Contents lists available at ScienceDirect

Bioorganic Chemistry

journal homepage: www.elsevier.com/locate/bioorg

Structure–activity relationship and biological evaluation of berberine derivatives as PCSK9 down-regulating agents

Tian-Yun Fan [1], Yu-Xin Yang [1], Qing-Xuan Zeng, Xue-Lei Wang, Wei Wei, Xi-Xi Guo, Li-Ping Zhao, Dan-Qing Song, Yan-Xiang Wang [*], Li Wang [*], Bin Hong [*]

Institute of Medicinal Biotechnology, Chinese Academy of Medical Science & Peking Union Medical College, Beijing 10050, China

ARTICLE INFO

Keywords:
PCSK9
Berberine
Structure–activity relationship
Transcriptional inhibition
LDL-C

ABSTRACT

Proprotein convertase subtilisin/kexin type 9 (PCSK9) is a secreted protein and its deficiency markedly enhanced the survival rate of patient with cardiovascular diseases (CVDs). Forty berberine (BBR) derivatives were synthesized and evaluated for their activities on down-regulating the transcription of PCSK9 in HepG2 cells, taking BBR as the lead. Structure–activity relationship (SAR) analysis revealed that 2,3-dimethoxy moiety might be beneficial for activity. Among them, **9k** displayed the most potent activity with IC_{50} value of 9.5 ± 0.5 μM, better than that of BBR. Also, it significantly decreased PCSK9 protein level at cellular level, as well as in the liver and serum of mice *in vivo*. Furthermore, **9k** markedly increased LDLR expression and LDL-C clearance via down-regulating PCSK9 protein. The mechanism of action of **9k** is targeting HNF1α and/or Sp1 cluster modulation upstream of PCSK9, a different one from BBR. Therefore, **9k** might have the potential to be a novel PCSK9 transcriptional inhibitor for the treatment of atherosclerosis, worthy for further investigation.

1. Introduction

Cardiovascular diseases (CVDs) are still a major cause of death worldwide [1]. Hepatic low-density lipoprotein receptor (LDLR) is a major target responsible for the removal of circulating low-density lipoprotein cholesterol (LDL-C), which is closely associated with the development of atherosclerosis [2,3]. Proprotein convertase subtilisin/kexin type 9 (PCSK9) is a secreted plasma protease that reduce hepatic LDLR protein level and induce increased plasma LDL-C levels by binding and shuttling LDLR to lysosomes for degradation. Clinically, deficiency of PCSK9 significantly improves the survival rate of patient with CVDs [4–6]. Thus, development of agents targeting PCSK9 expression or activity inhibition shows benefit in reducing the risk of cardiovascular disease. Two PCSK9-blocking monoclonal antibodies (alirocumab and evolocumab) have been successfully used in clinic alone or in combination with statin [7–10]. Besides, inclisiran, a novel siRNA-based PCSK9 silencer, has just been approved by the European Medicines Agency (EMA), which effectively sustains low density lipoprotein cholesterol (LDL-C) reduction by ~40% among patients with high risk of CVDs [11]. Since both the high cost of PCSK9 monoclonal antibodies and the subcutaneous administration limit their widespread use, development of small-molecule PCSK9 inhibitors with lower cost and ease of administration are conceptually attractive [12–14], and shed a light on the novel anti-atherosclerosis drug discovery.

However, the shallow interaction surface between PCSK9 and low density lipoprotein receptor (LDLR) makes it difficult to be targeted directly by small-molecule inhibitors [15]. Therefore, we have successfully established a cell-based high-throughput screening (HTS) model for human PCSK9 transcriptional down-regulators and identified an effective small-molecule PCSK9 inhibitor to profoundly reduce atherosclerosis progression *in vivo* [16].

In the past few years, our group has been dedicated to the discovery of innovate candidates from Traditional Chinese Medicine. The natural alkaloid berberine (BBR, Fig. 1) could decrease PCSK9 expression in a time- and dose-dependent manner through transcription factor HNF1α and SREBP, followed by increasing expression of LDLR as well as clearance of LDL-C [17–21]. Based on this, taking BBR as the lead, we carried out structural modification and optimization and constructed a set of BBR analogues to elucidate the comprehensive structure–activity relationship (SAR) for PCSK9 expression (Fig. 1) and discover novel modulators targeting PCSK9 transcriptional expression.

All the target compounds were evaluated by luciferase reporter-

* Corresponding authors.
E-mail addresses: wangyanxiang@imb.pumc.edu.cn (Y.-X. Wang), wangli_imb@163.com (L. Wang), binhong69@hotmail.com (B. Hong).
[1] These authors made equal contributions to the work.

https://doi.org/10.1016/j.bioorg.2021.104994
Received 15 February 2021; Received in revised form 19 April 2021; Accepted 12 May 2021
Available online 18 May 2021

based HTS assay, the representative compound was further confirmed on the regulation of hepatic PCSK9 *in vitro* and *in vivo*, followed by its effect on LDLR protein expression and mediated LDL-C clearance in cultured hepatic cells. Additionally, preliminary mechanism of representative compound was elucidated in this study.

2. Results and discussion

2.1. Synthesis

The synthetic routes of all the target compounds were presented in Schemes 1 and 2, taking commercially available substituted benzaldehydes or palmatine (PMT) as the starting materials. Among all target products, compounds **7a**–**s**, **9a**, **9b**, **9f**–**g**, **9i** and **9q** have been previously reported in our lab [22–27].

As presented in Scheme 2, demethylation on position 9 was first conducted under the influence of quaternary ammonium cation on PMT skeleton [25–28]. PMT was first heated at 195–210 °C for 30 min under vacuum and then acidified in concentrated HCl/ethanol (5/95 by vol) to obtain the key intermediate **8** with a free hydroxyl in a 78% yield after purification. Afterwards, taking K_2CO_3 as the base and CH_3CN as the solvent, compound **8** was reacted with substituted benzyl halide or halogenated hydrocarbons in the presence or absence of sodium iodide (NaI) as the catalyst. The mixture was stirred at 71 °C for 4–10 h, and target products **9a**–**u** were acquired in yields of 43–68%. All of the final compounds were purified by flash column chromatography on silica gel with using CH_2Cl_2/CH_3OH as eluent.

2.2. Pharmacological evaluation

2.2.1. SAR analysis for PCSK9 transcriptional activity in PCSK9p-Luc HepG2 cells

All the target derivatives (10 μg/mL) were initially examined for their PCSK9 transcription inhibitory activities using the luciferase reporter-based HTS assay in PCSK9p-Luc HepG2 cells established in our lab [16]. Structures and PCSK9 down-regulatory activities of the 40 analogues are displayed in Table 1.

Firstly, SAR was focused on the D ring, and compounds **7a**–**e** with various alkoxy and halogens on position 9, 10 or 11 were prepared and tested. As shown in Table 1, most of them showed suppressed potency with inhibition rates of no more than 35%, lower than that of BBR (56%). Then, SAR was moved to ring A, and **7f** and **7g** with dimethoxy on positions 2 and 3 instead of methylenedioxy exhibited comparable PCSK9 down-regulatory activity to BBR, which hinted that 2,3-dimethoxy might be helpful for potency.

Thus, a set of PMT analogues with 2,3-dimethoxy moiety were constructed and screened. It has been reported that substituent on position 9 might help maintain or improve potencies [28], structural modification at this position was first carried out. Fat rings including substituted benzyl groups and saturated carbocycles were introduced in order to improve their lipophilic property and bioavailability. Therefore, benzyl or various methylated benzyl groups were introduced on position 9 respectively, and **9b**–**d** displayed comparable potencies against PCSK9 compared with that of BBR. While large-volume alkyls on benzyl were attached, the PCSK9 transcriptional inhibition rates of **9e**–**g** went up to 83–98%, much better than that of BBR [16]. Instead of alkyl substituent, methoxy, trifloromethoxy and trifluomethylthio (**9h**–**k**) were attached on benzyl respectively. Among them, compound **9h** with one methoxy at *meta*-position of benzyl group gave a declined potency with an inhibitory rate of 28%. While 3′,5′-dimethoxy substituent was introduced, the activity on **9i** was lost completely. Compounds **9j** and **9k** displayed potent inhibitory activities with inhibition rates of 88% and 98%, which indicated that fluorine-containing substituent might be beneficial for the improvement on potency. Besides, various halogens, and electron withdrawing groups such as nitro, cyano and ester group were employed on benzyl, by which compounds **9l**–**q** were created. However, most of them lost their downregulatory potencies on PCSK9. Finally, derivatives with various saturated rings on position 9 were synthesized and assessed. Both compounds **9r** and **9u** with six-member ring could obviously down-regulate PCSK9 expression. These results suggested that lipophilic substituent might be helpful for PCSK9 down-regulating activity.

Meanwhile, when the dimethoxy moiety was moved to positions 3 and 4, the activity of **7h** and **7i** descended apparently. Furthermore, larger volume substituents including ethoxy and benzyloxy groups, as well as smaller volume hydroxyl were respectively attached to elucidate the SAR on ring A. Still, weakened potencies were detected on compounds **7j**–**q** with inhibition rates of –2 to 40%. Finally, compounds **7r** and **7s** with trimethoxy substituted on ring A displayed declined activity. These results suggested that 2,3-dimethoxy might also be beneficial for PCSK9 down-regulatory activity, taking BBR as the positive control.

Therefore, four compounds **9e**, **9k**, **9r** and **9u** with inhibitory rates above 90% were selected as active compounds for the further confirmation of PCSK9 inhibitory effects. The PCSK9p-Luc HepG2 cells were treated with these active compounds under different concentrations for 24 h respectively, and the luciferase activities were detected. As represented in Fig. 2A, these four compounds dose-dependently suppressed the PCSK9 promoter activity (structures shown in Fig. 2C). Especially, compounds **9e** and **9k** showed the moderate activity with respective IC_{50} value of 7.6 ± 1.1 μM and 9.5 ± 0.5 μM, which were lower than that of BBR (13.1 ± 0.6 μM) (Fig. 2B). Thus, the two derivatives were chosen as key compounds for further evaluations.

2.2.2. Preliminary safety evaluations for key compounds *9e* and *9k* in vitro and in vivo

The effects of compounds **9e** and **9k** on cell viability were further evaluated using MTT assay in HepG2 cells. The cells were treated with **9e** or **9k** under a series of concentrations for 24 h and the cell viability was determined. As depicted in Fig. 3, compound **9k** displayed a lower cytotoxicity than **9e** with median toxic concentration (TC_{50}) value of 61.1 μM. Thus, compound **9k** was selected as a representative compound for next step. Furthermore, we examined the acute toxicity of **9k** on Kunming mice. Compound **9k** was given orally in a single dose of 0, 250, 500, or 1,000 mg/kg, respectively. Then the body weight, survival and behavioral characteristics were monitored for seven days. The mice behaved well under the dose of up to 1,000 mg/kg, indicating a good *in vivo* safety feature of compound **9k** with the half-lethal dose (LD_{50}) value of over 1,000 mg/kg.

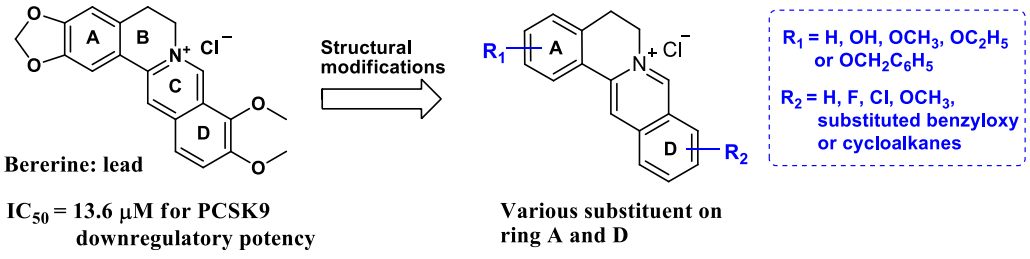

Fig. 1. Chemical structure of BBR and modification strategies.

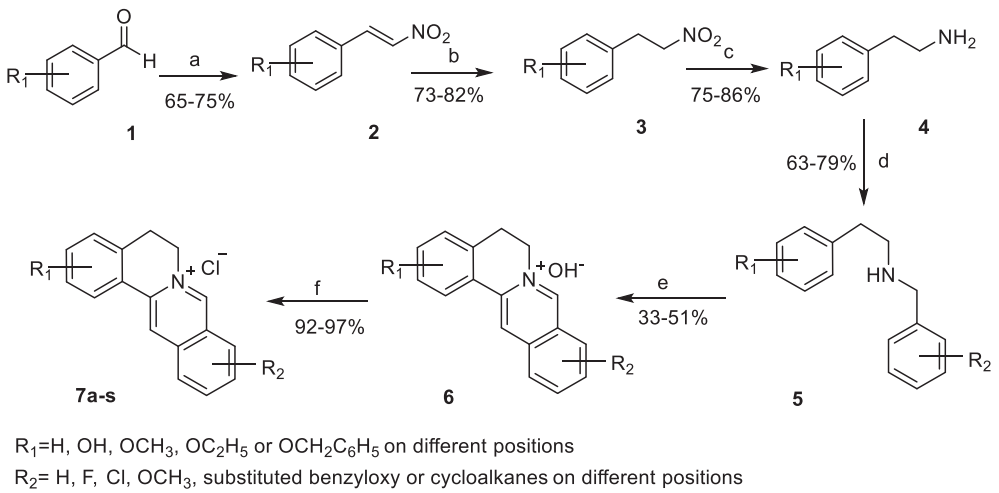

Scheme 1. Reagents and conditions: (a) CH_3NO_2, methanol, CH_3NH_2, 50 °C, 3.5 h; (b) $NaBH_4$, methanol, reflux, 2 h; (c) Zn, HCl, ethanol, 3 h; (d) 1) substituted of benzaldehyde, 100 °C, 8 h; 2) $NaBH_4$, methanol, reflux, 5 h; (e) glyoxal, formic acid, $CuSO_4$, HCl, 100 °C, 5 h; (f) 1) methanol/H_2O, CaO, rt, 2 h; 2) ethanol, HCl, rt, 0.5 h.

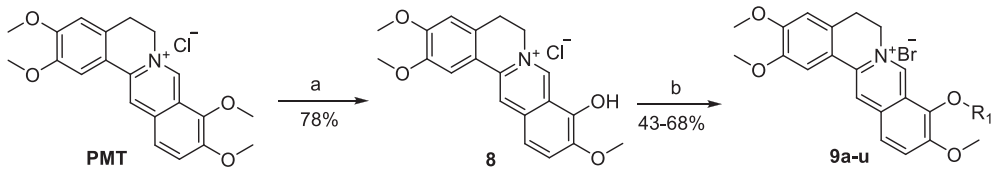

Scheme 2. Reagents and conditions: (**a**) 195–210 °C, 30–40 mmHg, 30 min.; (**b**) Substituted benzyl halide or halogenated hydrocarbons, K_2CO_3 for **9a**–**q** or K_2CO_3 and NaI for **9r**–**u**, CH_3CN, 71 °C, 4–10 h.

2.2.3. *Effects of **9k** on PCSK9 expression at protein level in vitro and in vivo*

To further validate the inhibitory activity of **9k** on PCSK9 expression, western blotting assay was applied to evaluate the effects on PCSK9 protein level in HepG2 cells firstly. The cells were treated with different concentrations of **9k** for 24 h, and PCSK9 protein level was detected. As shown in Fig. 4A, compound **9k** significantly decreased PCSK9 protein level even at the concentration of 5 μM. We further investigated the effect of **9k** on hepatic and serum PCSK9 content *in vivo*. Male C57BL/6J mice on standard chow diet in 2 groups (10 mice per group) were administrated with 50 mg/kg intragastrically every day for 4 weeks. Then the mice were sacrificed with 1% sodium pentobarbital, the liver and serum samples were collected individually to determine PCSK9 expression by western blotting and ELISA assay respectively. As showed in Fig. 4B, **9k** significantly decreased hepatic and serum PCSK9 protein level in C57BL/6J mice, which confirmed the effect of **9k** on PCSK9 expression *in vivo*.

2.2.4. *Effects of **9k** on LDLR expression and LDL cholesterol uptake in HepG2 cells*

Since PCSK9 could directly bind to LDLR and mediate its lysosomal degradation in hepatic cells, agents which lower PCSK9 protein level may also promote LDLR expression and increase LDL-C clearance [29,30]. Therefore, the effect of compound **9k** on LDLR expression was conducted in HepG2 cells. Compound **9k** with indicated concentrations was incubated with HepG2 cells for 24 h before LDLR protein level was detected by western blotting assay. As shown in Fig. 5A, **9k** significantly up-regulated LDLR protein levels in a dose-dependent manner, suggesting a potential role of **9k** in the regulation of LDLR mediated LDL-C uptake.

To further confirm whether the reduction of PCSK9 expression and the following LDLR increasement induced by **9k** could promote LDL-C clearance in HepG2 cells, 1,1′-dioctadecyl-3,3,3′,3′-tetramethylindocarbocyanine perchlorate-labeled LDL (DiI-LDL) uptake was conducted using flow cytometry analysis. HepG2 cells were treated with vehicle or different concentrations of **9k** for 24 h, then incubated with DiI-LDL (2 μg/mL) at 37 °C for 4 h before detection by flow cytometry. The results showed that **9k** treatment markedly promoted DiI-LDL uptake in a dose-dependent manner with a scale of 2–3 folds, which was much more effective than that of BBR (Fig. 5B, C), implying a dominant role of **9k** in regulating LDL-C metabolism. Besides, fluorescence visualization of DiI-LDL uptake by HepG2 cells was viewed by a Confocal Laser Scanning Microscope, which revealed a similar result that **9k** increased DiI-LDL-induced fluorescence accumulation in HepG2 cells (Fig. 5D). Taken together, these results suggested that **9k** is superior to BBR with better effect on LDL-C clearance.

2.2.5. *__9k__ transcriptionally reduced PCSK9 expression through HNF1α and Sp1modulation*

To investigate the mechanism involved in PCSK9 reduction mediated by **9k**, we analyzed the effect of **9k** on the transcriptional activity of PCSK9 promoter by transfection of HepG2 cells with the luciferase-reporter plasmids containing different truncated promoter region (D1–D7, Fig. 6A) of human PCSK9 gene [16]. The luciferase activity was detected after the incubation of **9k** with the HepG2 cells transfected with different individual construct. The results revealed that the luciferase activity of D1–D5 was significantly decreased by **9k**, which was markedly eliminated upon removal of the bases between −392 bp and −351 bp (D5 *vs.* D6, Fig. 6A). Besides, the inhibition effect of **9k** on D7 was abolished compared with pGL4 (D7 *vs.* pGL4, Fig. 6A). Taken together, all these results indicated that the regions between −392 bp and −351 bp (D5 *vs.* D6), −335 bp and −1 bp (D7 *vs.* pGL4) were both important for **9k** mediated PCSK9 transcriptional reduction, possibly associating with transcriptional factors HNF1α, HINFP or Sp1, rather than SREBP which is closely related to BBR [31]. There are two factors involved in the regions between −392 bp and −351 bp including HNF1α and HINFP.

Table 1

The structures and PCSK9 transcriptional activities of all target compounds (10 μg/mL) in HepG2 cells.

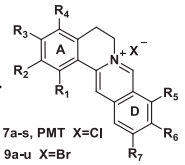

No.	R^1	R^2	R^3	R^4	R^5	R^6	R^7	Inhibition Rate (%)
BBR	H	OCH_2O		H	OCH_3	OCH_3	H	56
7a	H	OCH_2O		H	H	OCH_3	OCH_3	34
7b	H	OCH_2O		H	H	OCH_3	OC_2H_5	34
7c	H	OCH_2O		H	Cl	OCH_3	H	10
7d	H	OCH_2O		H	Cl	OCH_3	OCH_3	4
7e	H	OCH_2O		H	F	OCH_3	H	−9
7f	H	OCH_3	OCH_3	H	H	OCH_3	OCH_3	60
7g	H	OCH_3	OCH_3	H	H	OH	H	59
7h	H	H	OCH_3	OCH_3	OCH_3	OCH_3	H	24
7i	H	H	OCH_3	OCH_3	H	OCH_3	OCH_3	8
7j	H	OC_2H_5	OCH_3	H	OCH_3	OCH_3	H	19
7k	H	OC_2H_5	OCH_3	H	H	OCH_3	OCH_3	5
7l	H	OCH_3	OC_2H_5	H	OCH_3	OCH_3	H	9
7m	H	$C_6H_5CH_2O$	OCH_3	H	OCH_3	OCH_3	H	16
7n	H	H	OH	H	OCH_3	OCH_3	H	32
7o	H	H	OH	H	H	OCH_3	OCH_3	−2
7p	H	OCH_3	OH	H	H	OCH_3	OCH_3	40
7q	H	OH	OCH_3	H	H	OCH_3	OCH_3	36
7r	OCH_3	OCH_3	OCH_3	H	OCH_3	OCH_3	H	13
7s	H	OCH_3	OCH_3	OCH_3	OCH_3	OCH_3	H	22
PMT	H	OCH_3	OCH_3	H	OCH_3	OCH_3	H	38
9a	H	OCH_3	OCH_3	H	$C_6H_5CH_2O$	OCH_3	H	−11
9b	H	OCH_3	OCH_3	H	*p*-$CH_3C_6H_4CH_2O$	OCH_3	H	55
9c	H	OCH_3	OCH_3	H	*o*-$CH_3C_6H_4CH_2O$	OCH_3	H	67
9d	H	OCH_3	OCH_3	H	*3′,5′*-$(CH_3)_2C_6H_3CH_2O$	OCH_3	H	87
9e	H	OCH_3	OCH_3	H	*p*-$CH_3(CH_2)_3C_6H_4CH_2O$	OCH_3	H	98
9f	H	OCH_3	OCH_3	H	*p*-$C(CH_3)_3C_6H_4CH_2O$	OCH_3	H	83
9g	H	OCH_3	OCH_3	H		OCH_3	H	86
9h	H	OCH_3	OCH_3	H	*m*-$CH_3OC_6H_4CH_2O$	OCH_3	H	28
9i	H	OCH_3	OCH_3	H	*3′,4′*-$(CH_3O)_2C_6H_3CH_2O$	OCH_3	H	−9
9j	H	OCH_3	OCH_3	H	*p*-$CF_3OC_6H_4CH_2O$	OCH_3	H	88
9k	H	OCH_3	OCH_3	H	*p*-$SCF_3C_6H_4CH_2O$	OCH_3	H	98
9l	H	OCH_3	OCH_3	H	*2′,4′*-$F_2C_6H_3CH_2O$	OCH_3	H	26
9m	H	OCH_3	OCH_3	H	*3′,5′*-$F_2C_6H_3CH_2O$	OCH_3	H	37
9n	H	OCH_3	OCH_3	H	*p*-$CH_3OCOC_6H_4CH_2O$	OCH_3	H	−43
9o	H	OCH_3	OCH_3	H	*p*-$CNC_6H_4CH_2O$	OCH_3	H	−34
9p	H	OCH_3	OCH_3	H	*m*-$NO_2C_6H_4CH_2O$	OCH_3	H	−5
9q	H	OCH_3	OCH_3	H	*o*-$NO_2C_6H_4CH_2O$	OCH_3	H	19
9r	H	OCH_3	OCH_3	H		OCH_3	H	96
9s	H	OCH_3	OCH_3	H	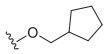	OCH_3	H	68
9t	H	OCH_3	OCH_3	H		OCH_3	H	8
9u	H	OCH_3	OCH_3	H	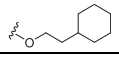	OCH_3	H	98

Thus, to further identify which factor plays a key role in **9k** mediated PCSK9 modulation, respective binding site in PCSK9 promoter was mutated. As shown in Fig. 6B, the inhibitory effect of **9k** on D5 was significantly abolished with missing HNF1α binding site, but not HINFP, implying that **9k** regulated PCSK9 mainly through HNF1α instead of HINFP, which was similar to BBR [31]. Meanwhile, beside HNF1α, Sp1 cluster might also take a part in **9k** induced PCSK9 reduction. In summary, **9k** might exert its effect on PCSK9 expression through HNF1α and/or Sp1 cluster, not exactly same as BBR.

3. Conclusions

Taken together, 40 BBR derivatives, of which 15 were new, were synthesized and screened for their activities on reduction of PCSK9 transcription in HepG2 cells. SAR study indicated that 2,3-dimethoxy moiety and introduction of a suitable substituent at position 9 might improve PCSK9 down-regulatory activity. Among them, **9k** displayed the most potent activity on expression of PCSK9 with IC_{50} value of 9.5 ± 0.5 μM, and exhibited good *in vivo* safety characters with LD_{50} value of over 1,000 mg/kg. Notably, **9k** significantly decreased PCSK9 protein level in vitro and *in vivo*. Most importantly, **9k** markedly increased LDL-C uptake in a dose-dependent manner through key PCSK9 protein. Preliminary mechanism research indicated that **9k** targeted transcription factor HNF1α and/or Sp1 cluster modulation to reduce PCSK9 expression, thereby enhance LDLR expression and LDL-C clearance, a different mechanism from BBR, suggesting a change in the mechanism of action after structural modifications. Therefore, **9k** might have the potential to be a novel PCSK9 down-regulatory agent for the treatment of cardiovascular diseases, worthy for further investigations.

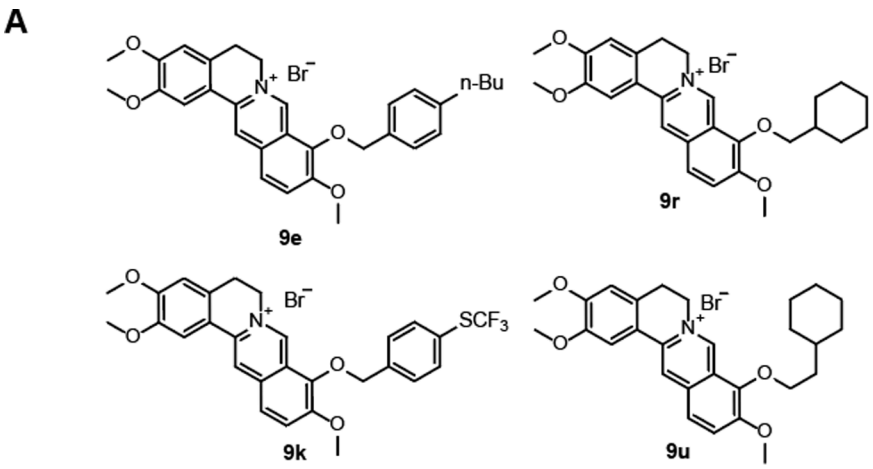

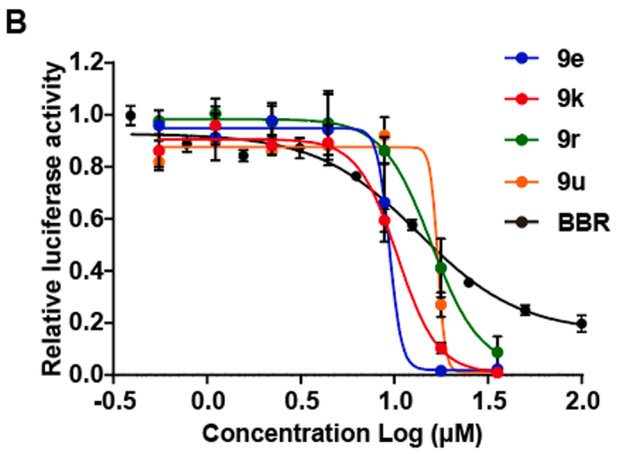

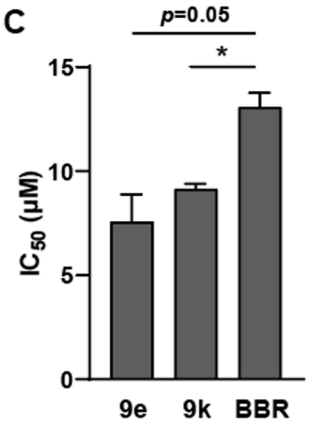

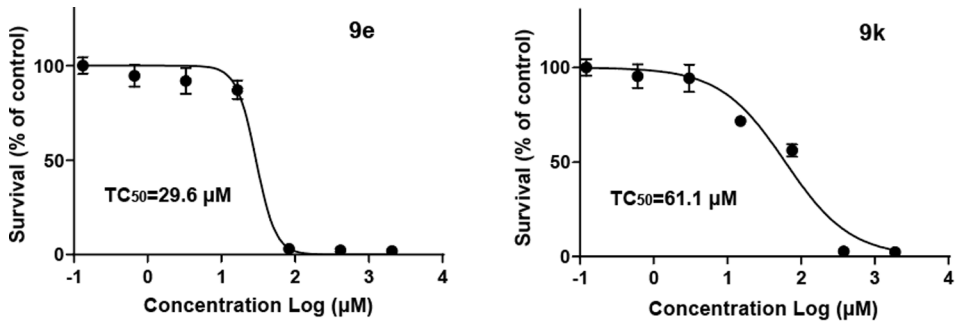

Fig. 2. Identification of active compounds through PCSK9 transcriptional inhibitor HTS assay and structures of representative compounds **9e**, **9k**, **9r**, **9u** and BBR. (A) Structures of compounds **9e**, **9k**, **9r**, **9u** (BBR: See Fig. 1.) (B) The dose–effect curves were drawn and the respective IC_{50} was calculated. Representative dose–effect curves are shown. Each concentration was replicated three times. (C) IC_{50} values of **9e**, **9k** and BBR are shown with bars as mean ± SEM from three independent experiments. $^{*}p < 0.05$.

Fig. 3. Cell toxicity of active compounds **9e** and **9k** was evaluated by MTT assay in HepG2 cells. The dose–effect curves were drawn and the respective TC_{50} was calculated. Each concentration was replicated three times.

4. Experimental section

4.1. General

Melting point (mp) was uncorrected using an MPA 100 OptiMelt automated melting point system (Stanford Research Systems, California, USA). The IR spectra were tested by Frontier FT-IR/NIR spectrometer using Spectrum 10 software (PerkinElmer Frontier, Massachusetts, USA). The ^{1}H and ^{13}C NMR spectra were performed on a Bruker Avance 600 MHz spectrometer (AV600-III, Bruker, Swiss) in DMSO-d_6 with Me_4Si as the internal standard. ESI high-resolution mass spectra (HRMS-ESI) were recorded on an Autospec UItima-TOF mass spectrometer (Micromass UK Ltd, Manchester, UK). Flash chromatography was performed on CombiflashRf 200 (Teledyne, Nebraska, USA), silica gel particle size 0.038 mm.

4.2. Chemistry

4.2.1. Synthesis procedure for compounds *7a–s, 9a, 9b, 9f–g, 9i* and *9q*

The synthetic methods and structural identification of compounds **7a–s**, **9a**, **9b**, **9f–g**, **9i** and **9q** have been previously reported in our lab [19–23].

4.2.2. General synthesis procedure for compounds *9c–e, 9h, 9j–p, 9r–u*

PMT (3.87 g, 10 mmol) was heated at 195–210 °C for 30 min under vacuum (20–30 mmHg), and then a dark purple solid was obtained.

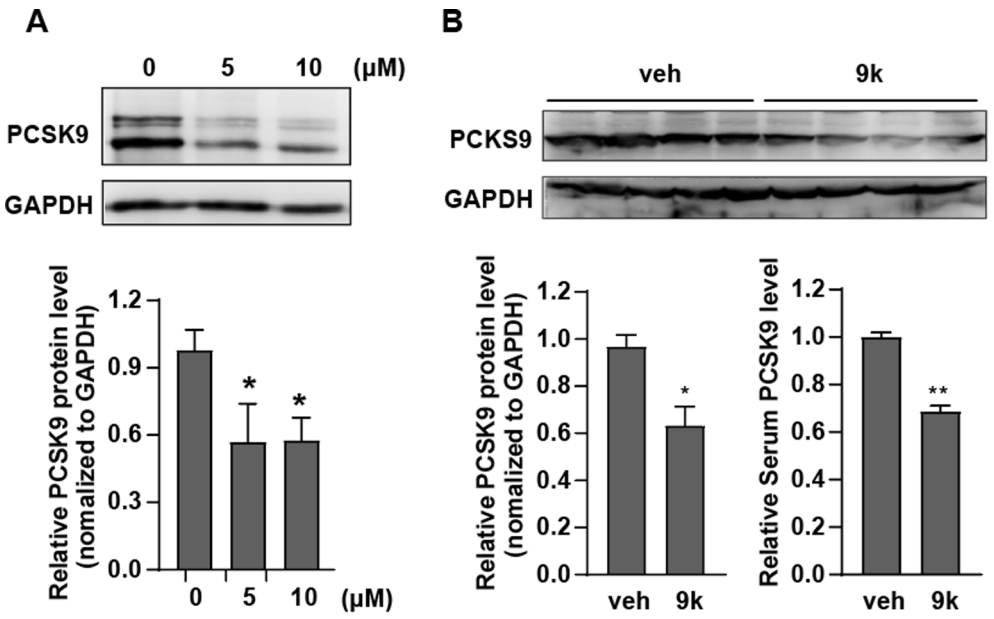

Fig. 4. Effects of **9k** on PCSK9 expression in HepG2 cells and C57BL/6J mice. (A) Western blotting assay for **9k**-regulated PCSK9 protein level. Representative images are shown. Gray scanning analysis was performed from 3 independent experiments. (B) Male C57BL/6 mice were intragastrically administrated with vehicle (veh) or **9k** (50 mg/kg). At the end of experiment, liver samples and serum were collected and PCSK9 protein level was detected. Data are shown as mean ± SEM. $*p < 0.05$, $**p < 0.01$, $***p < 0.001$ *vs.* vehicle group.

After the solid was cooled to room temperature, ethanol/concentrated HCl (95/5) were added and the yellow solution was acquired. Then, after the solvent was removed, the remaining residue was purified by flash chromatography while using CH_2Cl_2/CH_3OH as the gradient eluent to obtain the intermediate **8** (3.43 g, 80%) as a brown solid.

Compound **8** (100 mg, 0.40 mmol), K_2CO_3 (1.60 mmol) with or without NaI (1.60 mmol) were added in anhydrous DMF (6 mL), and the mixture was stirred for 10 min at room temperature. Afterwards, corresponding benzyl halides (1.60 mmol) or halogenated hydrocarbons (1.60 mmol) were added, and the mixture was heated at 71 °C for 4–10 h, and then filtered. The resulting residue was acidified with concentrated HCl/ethanol (5:95 by vol.), purified through flash chromatography on silica gel using CH_2Cl_2/CH_3OH as the gradient eluent to acquire the desired compounds **9c**–**e**, **9h**, **9j**–**p**, **9r**–**u**.

*4.2.2.1. 2,3,10-Trimethoxy-9-o-methylbenzyloxyprotopalmatine bromide (**9c**).* Brown solid; yield: 24%; mp: 164–166 °C; IR: 3405, 2920, 1512, 1359, 1272, 1106, 1018, 744 cm^{-1}; ^1H NMR: δ 9.59 (s, 1H), 9.07 (s, 1H), 8.24 (dd, $J = 9.0$, 3.6 Hz, 1H), 8.08 (d, $J = 9.0$ Hz, 1H), 7.72 (s, 1H), 7.56 (d, $J = 9.0$ Hz, 1H), 7.49–7.17 (m, 3H), 7.10 (s, 1H), 5.35 (s, 2H), 4.90 (t, $J = 6.6$ Hz, 2H), 4.07 (s, 3H), 3.94 (s, 3H), 3.87 (s, 3H), 3.21 (t, $J = 6.6$ Hz, 2H), 2.45 (s, 3H); ^{13}C NMR δ 151.5, 150.8, 148.7, 145.2, 142.2, 137.6, 136.7, 134.7, 133.1, 130.1, 129.5, 128.6, 128.5, 126.6, 125.8, 123.8, 121.7, 112.0, 118.8, 111.3, 108.8, 73.5, 57.0, 56.2, 55.9, 55.7, 26.0, 18.6; HRMS: calcd for $C_{28}H_{28}NO_4Br$ $[M-Br]^+$: 442.2013, found: 442.2012.

*4.2.2.2. 2,3,10-Trimethoxy-9-3′,5′-dimethylbenzyloxyprotopalmatine bromide (**9d**).* Brown solid; yield: 46%; mp: 191–193 °C; IR: 3466, 2973, 1608, 1359, 1276, 1110, 822, 705 cm^{-1}; ^1H NMR: δ 9.72 (s, 1H), 9.06 (s, 1H), 8.24 (dd, $J = 9.0$, 2.4 Hz, 1H), 8.06 (d, $J = 9.0$ Hz, 1H), 7.72 (s, 1H), 7.19 (d, $J = 10.8$ Hz, 2H), 7.10 (s, 1H), 6.99 (s, 1H), 5.26 (s, 2H), 4.94 (t, $J = 6.6$ Hz, 2H), 4.10 (d, $J = 1.8$ Hz, 3H), 3.94 (d, $J = 1.2$ Hz, 3H), 3.87 (d, $J = 1.8$ Hz, 3H), 3.22 (t, $J = 6.6$ Hz, 2H), 2.29 (s, 6H); ^{13}C NMR: δ 151.5, 150.7, 148.7, 145.3, 142.1, 137.6, 137.4 (2), 136.3, 133.0, 130.8, 129.7, 128.6, 126.5 (2), 123.7, 121.8, 119.9, 118.9, 111.3, 108.7, 75.5, 57.0, 56.2, 55.9, 55.5, 26.0, 20.9 (2); HRMS: calcd for $C_{29}H_{30}NO_4Br$ $[M-Br]^+$: 456.2169, found: 456.2169.

*4.2.2.3. 2,3,10-Trimethoxy-9-p-(n-butyl)benzyloxyprotopalmatine bromide (**9e**).* Yellow solid; yield: 57%; mp: 215–217 °C; IR: 3397, 2937, 1602, 1509, 1357, 1275, 1022, 873 cm^{-1}; ^1H NMR: δ 9.69 (s, 1H), 9.00 (s, 1H), 8.22 (d, $J = 9.0$ Hz, 1H), 8.02 (d, $J = 9.0$ Hz, 1H), 7.70 (s, 1H), 7.47 (d, $J = 7.8$ Hz, 2H), 7.20 (d, $J = 7.8$ Hz, 2H), 7.10 (s, 1H), 5.31 (s, 2H), 4.91 (t, $J = 6.6$ Hz, 2H), 4.10 (s, 3H), 3.93 (s, 3H), 3.87 (s, 3H), 3.21 (t, $J = 6.6$ Hz, 2H), 2.56 (t, $J = 7.8$ Hz, 2H), 1.54–1.45 (m, 2H), 1.32–1.10 (m, 2H), 0.83 (t, $J = 7.2$ Hz, 3H); ^{13}C NMR: δ 151.5, 150.7, 148.7, 145.4, 142.7, 141.9, 137.5, 133.6, 133.0, 129.0 (2), 128.6, 128.2 (2), 126.6, 123.6, 121.9, 119.8, 118.9, 111.3, 108.7, 75.2, 57.0, 56.1, 55.9, 55.5, 34.5, 33.1, 26.0, 21.6, 13.7; HRMS: calcd for $C_{31}H_{34}NO_4Br$ $[M-Br]^+$: 484.2482, found: 484.2483.

*4.2.2.4. 2,3,10-Trimethoxy-9-m-methoxylbenzyloxyprotopalmatine bromide (**9h**).* Faint yellow solid; yield: 33%; mp: 179–181 °C; IR: 3451, 2960, 1608, 1511, 1241, 1110, 870, 779 cm^{-1}; ^1H NMR: δ 9.77 (s, 1H), 9.05 (s, 1H), 8.23 (d, $J = 9.0$ Hz, 1H), 8.05 (d, $J = 9.0$ Hz, 1H), 7.72 (s, 1H), 7.30 (t, $J = 7.8$ Hz, 1H), 7.19 (s, 1H), 7.13 (d, $J = 7.8$ Hz, 1H), 7.10 (s, 1H), 6.91 (dd, $J = 8.4$, 2.4 Hz, 1H), 5.34 (s, 2H), 4.94 (t, $J = 6.6$ Hz, 2H), 4.10 (s, 3H), 3.94 (s, 3H), 3.88 (s, 3H), 3.77 (s, 3H), 3.22 (t, $J = 6.6$ Hz, 2H); ^{13}C NMR: δ 159.3, 151.5, 150.5, 148.7, 145.3, 141.9, 137.9, 137.6, 133.0, 129.4, 128.6, 126.6, 123.6, 121.8, 120.8, 119.9, 118.8, 114.1, 114.0, 111.3, 108.8, 75.2, 57.0, 56.2, 55.6, 55.5, 55.1, 26.0; HRMS: calcd for $C_{28}H_{28}NO_5Br$ $[M-Br]^+$: 458.1962, found: 458.1966.

*4.2.2.5. 2,3,10-Trimethoxy-9-p-trifluoromethoxybenzyloxyprotopalmatine bromide (**9j**).* Faint yellow solid; yield: 38%; mp: 187–189 °C; IR: 3400, 2982, 2610, 1607, 1359, 1276, 1110, 809 cm^{-1}; ^1H NMR: δ 9.83 (s, 1H), 9.07 (s, 1H), 8.24 (d, $J = 9.0$ Hz, 1H), 8.07 (d, $J = 9.0$ Hz, 1H), 7.86 (d, $J = 8.4$ Hz, 2H), 7.81 (d, $J = 8.4$ Hz, 2H), 7.73 (s, 1H), 7.11 (s, 1H), 5.46 (s, 2H), 4.96 (t, $J = 6.6$ Hz, 2H), 4.08 (s, 3H), 3.94 (s, 3H), 3.87 (s, 3H), 3.23 (t, $J = 6.6$ Hz, 2H); ^{13}C NMR: δ 151.5, 150.4, 148.7, 145.3, 141.8, 141.4, 137.7, 133.1, 128.9 (2), 128.7, 128.6, 126.6, 125.2 (2), 124.2, 123.8, 121.5, 119.9, 118.9, 111.3, 108.8, 74.4, 57.1, 56.2, 55.9, 55.5, 26.0; HRMS: calcd for $C_{28}H_{25}NO_5F_3Br$ $[M-Br]^+$: 512.1679, found: 512.1685.

*4.2.2.6. 2,3,10-Trimethoxy-9-p-trifluomethylthiobenzyloxyprotopalmatine bromide (**9k**).* Brown solid; yield: 47%; mp: 182–184 °C; IR: 3382, 2980, 1606, 1360, 1275, 1108, 1018, 812 cm^{-1}; ^1H NMR: δ 9.84 (s, 1H), 9.07 (s, 1H), 8.24 (d, $J = 9.0$ Hz, 1H), 8.07 (d, $J = 9.0$ Hz, 1H), 7.79 (s, 4H), 7.72 (s, 1H), 7.11 (s, 1H), 5.42 (s, 2H), 4.95 (t, $J = 6.6$ Hz, 2H), 4.07 (s, 3H), 3.94 (s, 3H), 3.87 (s, 3H), 3.23 (t, $J = 6.6$ Hz, 2H); ^{13}C NMR: δ 151.5, 150.4, 148.7, 145.3, 141.8, 140.3, 137.7, 136.1 (2), 133.1,

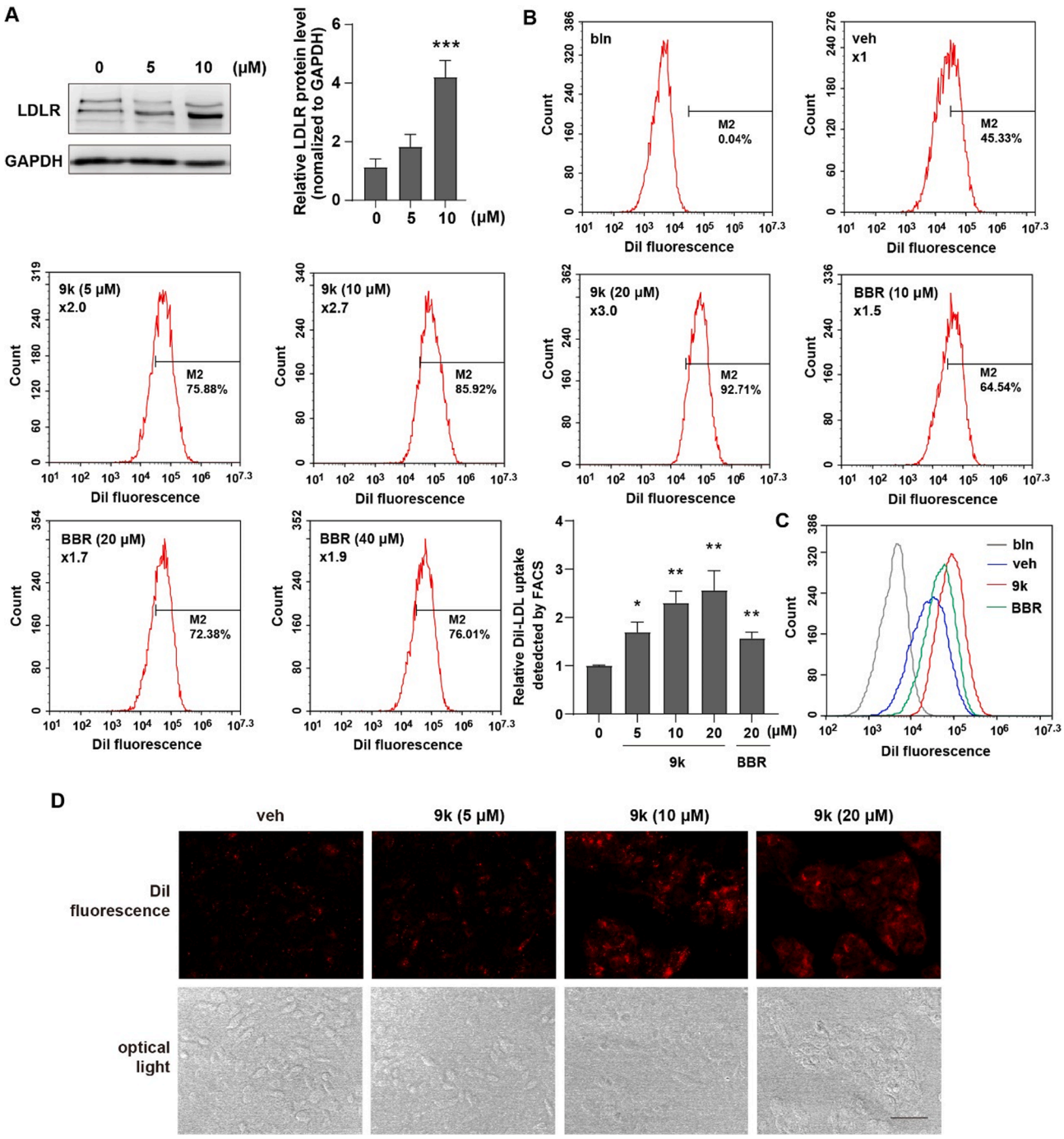

Fig. 5. Effects of **9k** on LDLR expression and LDL-C uptake in HepG2 cells. (A) Western blotting assay for LDLR protein level regulated by **9k**. Gray scanning analysis was performed from 3 independent experiments. (B) Flow cytometric analysis was conducted to detect LDL-C uptake. Representative images are shown and statistical analysis is performed from 3 independent experiments. (C) Overlay graph of blank (bln), vehicle (veh), **9k** (20 μM) and BBR (20 μM). (D) Fluorescence microscopy was used to analyze DiI uptake by HepG2 cells. Representative images are shown. Scale bar, 50 μm. The data are shown as mean ± SEM. $^{*}p < 0.05$, $^{**}p < 0.01$, $^{***}p < 0.001$ *vs.* vehicle group.

130.10, 129.6 (3), 126.5, 123.9, 122.7, 121.5, 119.9, 118.8, 111.3, 108.8, 74.3, 57.0, 56.2, 55.8, 55.5, 25.9; HRMS: calcd for $C_{28}H_{25}NO_4F_3SBr$ $[M-Br]^+$: 528.1451, found: 528.1448.

*4.2.2.7. 2,3,10-Trimethoxy-9-2′,4′-difluorobenzyloxyprotopalmatine bromide (**9l**).* Heavy brown solid; yield: 41%; mp: 187–189 °C; IR: 3008, 1603, 1507, 1363, 1215, 1023, 865, 726 cm^{-1}; ^1H NMR: δ 9.69 (s, 1H), 9.06 (s, 1H), 8.23 (d, $J = 9.0$ Hz, 1H), 8.07 (d, $J = 9.0$ Hz, 1H), 7.83–7.76 (m, 1H), 7.72 (s, 1H), 7.30 (td, $J = 9.6$, 2.4 Hz, 1H), 7.16 (td, $J = 8.4$, 2.4 Hz, 1H), 7.11 (s, 1H), 5.41 (s, 2H), 4.93 (t, $J = 6.6$ Hz, 2H), 4.06 (s, 3H), 3.94 (s, 3H), 3.87 (s, 3H), 3.22 (t, $J = 6.6$ Hz, 2H); ^{13}C NMR: δ 162.5, 160.8, 151.5, 150.6, 148.7, 145.1, 141.5, 137.7, 133.1, 133.0, 128.6, 126.6, 123.9, 121.6, 120.0 (2), 118.9, 111.6, 111.3, 108.8, 104.0, 68.5, 57.0, 56.2, 55.9, 55.6, 26.0; HRMS: calcd for $C_{27}H_{24}NO_4F_2Br$ $[M-Br]^+$: 464.1668, found: 464.1665.

*4.2.2.8. 2,3,10-Trimethoxy-9-3′,5′-difluorobenzyloxyprotopalmatine bromide (**9m**).* Yellow solid; yield: 42%; mp: 245–247 °C; IR: 2986, 1608, 1359, 1276, 1106, 1023, 866, 696 cm^{-1}; ^1H NMR: δ 9.85 (s, 1H), 9.06 (s, 1H), 8.24 (d, $J = 9.0$ Hz, 1H), 8.07 (d, $J = 9.0$ Hz, 1H), 7.72 (s, 1H),

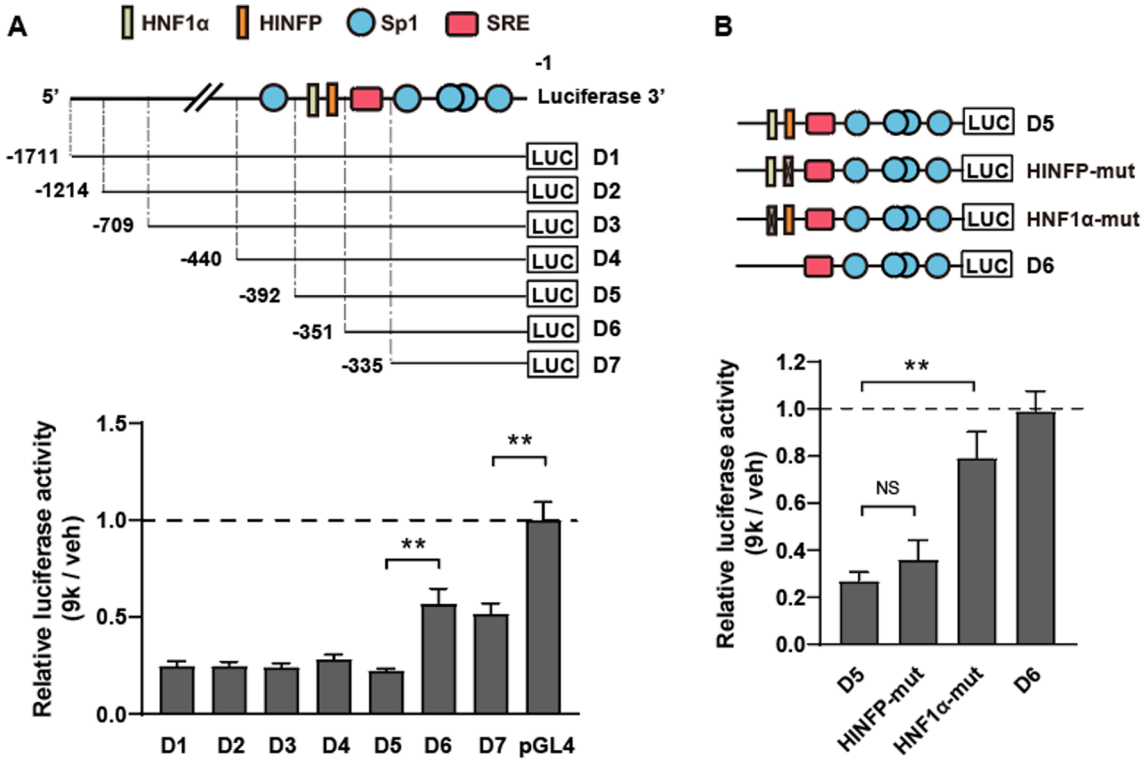

Fig. 6. **9k** downregulates PCSK9 transcriptional expression through HNF1α and Sp1 cluster. (A) Effects of **9k** on PCSK9 luciferase-reporter plasmids containing different truncated promoter region D1–D7 in HepG2 cells. Position −1 was the 3′ end of PCSK9 promoter inserts. HepG2 cells were transfected with the D1–D7 or pGL4 plasmids for 24 h and treated with vehicle or **9k** (10 μM) for 24 h. Then the luciferase activity was detected. (B) Mutation analysis of core nucleotide sequence of HNF1α or HINFP binding site in PCSK9 promoter. Data are shown as mean ± SEM (at least 3 independent experiments). $^{**}p < 0.01$ *vs.* vehicle group.

7.45–7.33 (m, 2H), 7.27 (td, J = 9.0, 2.4 Hz, 1H), 7.11 (s, 1H), 5.37 (s, 2H), 4.96 (t, J = 6.6 Hz, 2H), 4.08 (s, 3H), 3.94 (s, 3H), 3.88 (s, 3H), 3.23 (t, J = 6.6 Hz, 2H); ^{13}C NMR: δ 162.3 (2), 151.5, 150.4, 148.7, 145.3, 141.6, 141.1, 137.8, 133.1, 128.7, 126.6, 123.9, 121.5, 119.9, 118.9, 111.3 (2), 111.1, 108.8, 103.5, 73.7, 57.1, 56.2, 55.9, 55.5, 26.0; HRMS: calcd for $C_{27}H_{24}NO_4F_2Br$ $[M-Br]^+$: 464.1668, found: 464.1666.

*4.2.2.9. 2,3,10-Trimethoxy-9-p-carbomethoxybenzyloxyprotopalmatine bromide (**9n**).* Brown solid; yield: 39%; mp: 211–213 °C; IR: 3421, 2916, 1716, 1363, 1272, 1110, 866, 757 cm^{-1}; ^{1}H NMR: δ 9.82 (s, 1H), 9.05 (s, 1H), 8.23 (d, J = 9.0 Hz, 1H), 8.06 (d, J = 9.0 Hz, 1H), 8.03–7.98 (m, 2H), 7.76 (d, J = 7.8 Hz, 2H), 7.72 (s, 1H), 7.11 (s, 1H), 5.45 (s, 2H), 4.95 (t, J = 6.6 Hz, 2H), 4.08 (s, 3H), 3.94 (s, 3H), 3.87 (s, 3H), 3.86 (s, 3H), 3.22 (t, J = 6.6 Hz, 2H); ^{13}C NMR: δ 166.4, 152.0, 150.8, 149.2, 145.7, 142.5, 142.2, 138.2, 133.5, 129.8, 129.7 (2), 129.1, 128.9 (2), 127.0, 124.2, 122.0, 120.4, 119.3, 111.7, 109.2, 75.0, 57.5, 56.6, 56.3, 56.0, 52.7, 26.4; HRMS: calcd for $C_{29}H_{28}NO_6Br$ $[M-Br]^+$: 486.1911, found: 486.1911.

*4.2.2.10. 2,3,10-Trimethoxy-9-p-cyanobenzyloxyprotopalmatine bromide (**9o**).* Yellow solid; yield: 51%; mp: 198–200 °C; IR: 3387, 2982, 2227, 1603, 1359, 1276, 1110, 822 cm^{-1}; ^{1}H NMR: δ 9.83 (s, 1H), 9.06 (s, 1H), 8.24 (d, J = 9.0 Hz, 1H), 8.07 (d, J = 9.0 Hz, 1H), 7.94–7.87 (m, 2H), 7.87–7.76 (m, 2H), 7.72 (s, 1H), 7.11 (s, 1H), 5.45 (s, 2H), 4.95 (t, J = 6.6 Hz, 2H), 4.07 (s, 3H), 3.94 (s, 3H), 3.87 (s, 3H), 3.23 (t, J = 6.6 Hz, 2H); ^{13}C NMR: δ 151.5, 150.3, 148.7, 145.3, 142.3, 141.7, 137.8, 133.1, 132.4 (2), 128.9 (2), 128.6, 126.6, 123.9, 121.5, 119.9, 118.9, 118.7, 111.3, 110.9, 108.8, 74.3, 57.1, 56.2, 55.9, 55.5, 26.0; HRMS: calcd for $C_{28}H_{25}N_2O_4Br$ $[M-Br]^+$: 453.1809, found: 453.1809.

*4.2.2.11. 2,3,10-Trimethoxy-9-m-nitrobenzyloxyprotopalmatine bromide (**9p**).* Yellow solid; yield: 37%; mp: 230–232 °C; IR: 2920, 1607, 1525, 1350, 1215, 1114, 1018, 735 cm^{-1}; ^{1}H NMR: δ 9.89 (s, 1H), 9.07 (s, 1H), 8.51 (t, J = 1.8 Hz, 1H), 8.25 (d, J = 9.0 Hz, 2H), 8.08 (t, J = 9.0 Hz, 2H), 7.78–7.66 (m, 2H), 7.11 (s, 1H), 5.49 (s, 2H), 4.96 (t, J = 6.6 Hz, 2H), 4.09 (s, 3H), 3.94 (s, 3H), 3.87 (s, 3H), 3.23 (t, J = 6.6 Hz, 2H); ^{13}C NMR: δ 152.0, 150.9, 149.2, 148.2, 145.8, 142.1, 139.3, 138.2, 135.4, 133.5, 130.5, 129.1, 126.9, 124.5, 123.6, 123.4, 122.0, 120.4, 119.3, 111.7, 109.2, 74.5, 57.5, 56.6, 56.3, 55.9, 26.4; HRMS: calcd for $C_{27}H_{25}N_2O_6Br$ $[M-Br]^+$: 473.1707, found: 473.1705.

*4.2.2.12. 2,3,10-Trimethoxy-9-cyclohexylmethoxyprotopalmatine bromide (**9r**).* Yellow solid; yield: 45%; mp: 260–262 °C; IR: 2930, 1606, 1524, 1360, 1278, 1115, 1022, 879 cm^{-1}; ^{1}H NMR: δ 9.66 (d, J = 2.4 Hz, 1H), 9.04 (s, 1H), 8.20 (dd, J = 9.0, 2.4 Hz, 1H), 8.02 (d, J = 9.0 Hz, 1H), 7.71 (d, J = 1.8 Hz, 1H), 7.11 (d, J = 1.8 Hz, 1H), 4.96 (t, J = 6.6 Hz, 2H), 4.10 (d, J = 6.6 Hz, 2H), 4.05 (d, J = 1.8 Hz, 3H), 3.94 (d, J = 1.8 Hz, 3H), 3.87 (d, J = 1.8 Hz, 3H), 3.23 (t, J = 6.6 Hz, 2H), 2.05–1.84 (m, 1H), 1.81–1.66 (m, 4H), 1.42–1.01 (m, 6H); ^{13}C NMR: δ 151.5, 150.2, 148.7, 145.1, 143.0, 137.6, 133.2, 128.6, 126.8, 123.1, 121.4, 119.9, 118.9, 111.3, 108.7, 79.4, 57.1, 56.2, 55.9, 55.7, 37.9, 29.2 (2), 26.1, 26.0, 25.3 (2); HRMS: calcd for $C_{27}H_{32}NO_4Br$ $[M-Br]^+$: 434.2326, found: 434.2326.

*4.2.2.13. 2,3,10-Trimethoxy-9-cyclopentylmethoxylprotopalmatine bromide (**9s**).* Faint yellow solid; yield: 39%; mp: 234–236 °C; IR: 3392, 2920, 1603, 1359, 1241, 1114, 1018, 861 cm^{-1}; ^{1}H NMR: δ 9.69 (s, 1H), 9.04 (s, 1H), 8.20 (d, J = 9.0 Hz, 1H), 8.03 (d, J = 9.0 Hz, 1H), 7.72 (s, 1H), 7.10 (s, 1H), 4.97 (t, J = 6.6 Hz, 2H), 4.18 (d, J = 7.2 Hz, 2H), 4.05 (s, 3H), 3.94 (s, 3H), 3.87 (s, 3H), 3.23 (t, J = 6.6 Hz, 2H), 2.04–1.94 (m, 1H),1.90–1.79 (m, 2H), 1.69–1.53 (m, 4H), 1.50–1.38 (m, 2H); ^{13}C NMR: δ 151.5, 150.2, 148.7, 145.2, 142.8, 137.6, 133.1, 128.6, 126.7, 123.1, 121.5, 119.9, 118.9, 111.3, 108.7, 78.3, 57.0, 56.2, 55.9, 55.6, 39.6, 29.0 (2), 26.0, 25.1 (2); HRMS: calcd for $C_{26}H_{30}NO_4Br$ $[M-Br]^+$: 420.2169, found: 420.2170.

*4.2.2.14. 2,3,10-Trimethoxy-9-cyclobutylmethoxylprotopalmatine bromide (**9t**).* Yellow solid; yield: 47%; mp: 237–239 °C; IR: 3392, 2977, 2231, 1608, 1511, 1359, 1110, 866 cm^{-1}; ^1H NMR: δ 9.69 (s, 1H), 9.03 (s, 1H), 8.20 (d, $J = 9.0$ Hz, 1H), 8.03 (d, $J = 9.0$ Hz, 1H), 7.71 (s, 1H), 7.10 (s, 1H), 4.96 (t, $J = 6.6$ Hz, 2H), 4.29 (d, $J = 7.20$ Hz, 2H), 4.06 (s, 3H), 3.94 (s, 3H), 3.87 (s, 3H), 3.23 (t, $J = 6.6$ Hz, 2H), 2.88 (p, $J = 7.2$ Hz, 1H), 2.16–2.02 (m, 2H), 1.99–1.88 (m, 4H); ^{13}C NMR: δ 151.5, 150.3, 148.7, 145.1, 142.7, 137.7, 133.1, 128.6, 126.7, 123.2, 121.6, 119.9, 118.9, 111.3, 108.7, 78.0, 57.0, 56.2, 55.9, 55.6, 34.6, 26.0, 24.5 (2), 18.1; HRMS: calcd for $C_{25}H_{28}NO_4Br$ $[M-Br]^+$: 406.2013, found: 406.2012.

*4.2.2.15. 2,3,10-Trimethoxy-9–2′-cyclohexylethyoxylprotopalmatine bromide (**9u**).* Faint yellow solid; yield: 32%; mp: 204–206 °C; IR: 3390, 2920, 1606, 1360, 1275, 1111, 1019, 812 cm^{-1}; ^1H NMR: δ 9.74 (s, 1H), 9.04 (d, $J = 3.0$ Hz, 1H), 8.20 (dd, $J = 9.0$, 2.4 Hz, 1H), 8.03 (d, $J = 9.0$ Hz, 1H), 7.72 (s, 1H), 7.10 (d, $J = 1.8$ Hz, 1H), 4.97 (t, $J = 6.6$ Hz, 2H), 4.33 (td, $J = 6.6$, 1.8 Hz, 2H), 4.05 (d, $J = 1.8$ Hz, 3H), 3.94 (d, $J = 1.2$ Hz, 3H), 3.87 (d, $J = 1.8$ Hz, 3H), 3.23 (t, $J = 6.6$ Hz, 2H), 1.79–0.93 (m, 13H); ^{13}C NMR: δ 151.5, 150.2, 148.7, 145.3, 142.8, 137.6, 133.1, 128.6, 126.7, 123.2, 121.6, 119.9, 118.9, 111.3, 108.7, 72.3, 57.0, 56.2, 55.9, 55.5, 36.8, 33.9, 32.8 (2), 26.1, 26.0, 25.8 (2); HRMS: calcd for $C_{28}H_{34}NO_4Br$ $[M-Br]^+$: 448.2482, found: 448.2478.

4.3. Biological methods

4.3.1. Cells and animals

The human hepatoma cell line HepG2 cells were cultured in Eagle minimal essential medium (MEM, Invitrogen, Carlsbad, USA) supplemented with 10% fetal bovine serum (FBS, Gibco, Grand Island, USA), 1% nonessential amino acids and 1% sodium pyruvate (Invitrogen).

The stable pGL4-PCSK9-P transfected HepG2 cells, named as PCSK9p-Luc HepG2 cells and used as PCSK9 transcriptional inhibitor HTS assay [12], were cultured in MEM supplemented with 10% FBS, 1% nonessential amino acids, 1% sodium pyruvate and additional G418 (700 mg/mL, Invitrogen). Cells were maintained at 37 °C in the presence of 5% CO_2.

All experimental procedures relating animals were approved by the Institutional Laboratory Animal Care and Use Committee of Institute of Medicinal Biotechnology. Kunming mice and C57BL/6J mice were purchased from Vital River Laboratory Animal Technology (Beijing, China). Kunming mice with body weights of 20.0 ± 1.0 g were fed regular rodent chow diet and randomly divided into four groups with six mice each. Compound **9k** was given orally in a single dose of 0, 250, 500, or 1,000 mg/kg, respectively. Then the body weight, survival and behavioral characteristics were monitored for seven days. C57BL/6J mice (~8 weeks old) were used to investigate the effect of **9k** on PCSK9 expression *in vivo*, which were divided into 2 groups (10 mice/group) intragastric administrated with **9k** (50 mg/kg) or vehicle every day for 4 weeks. Mice were sacrificed, and serum and liver samples were collected for further determination of PCSK9 by western blotting assay.

4.3.2. Screening

The PCSK9p-Luc HepG2 cells cultured in MEM medium were treated with different compounds at a concentration of 10 μg/mL or 0.1% DMSO for 24 h. The luciferase activities were measured by the Luciferase Assay System (Promega, Madison, USA) and detected using a Victor X5 multilabel plate reader (PerkinElmer, Waltham, USA). Then the inhibitory rates were calculated as percentage.

4.3.3. MTT assay

Compounds **9e** and **9k** were added to HepG2 cells for 24 h and then MTT reagent (1 mg/mL) was added and incubated at 37 °C for 4 h, using MTT assay. Cells were washed and added with DMSO to dissolve the purple formazan crystals, and the absorbance at 550 nm was measured using a Victor X5 multilabel plate reader (PerkinElmer, Waltham, MA, USA).

4.3.4. Western blotting assay

HepG2 cells plated in 12-well plate were treated with compound **9k** in MEM for 24 h. Then the cells were lysed using RIPA lysis buffer (Applygen, Beijing, China). The lysed protein samples were separated using 10% SDS-polyacrylamide gel electrophoresis (PAGE), then electroblotted onto a 0.45 μm polyvinylidene fluoride (PVDF) membrane (Millipore, Bedford, USA). The PVDF membranes were then incubated with primary antibodies against PCSK9 (R&D Systems, Minneapolis, USA), LDLR (Abcam, Cambridge, UK) or GAPDH (ZSJQ-Bio, Beijing, China) at 4 °C overnight. The membranes were washed and incubated with horse radish peroxidase (HRP)-conjugated secondary antibodies (ZSJQ-Bio) at room temperature for 1 h. All bands were visualized with an enhanced chemiluminescence detection system (Millipore). Image J software was used to quantify PCSK9 or LDLR protein amounts, normalized to GAPDH.

4.3.5. DiI-LDL uptake assay

HepG2 cells were treated with **9k** as described above. One day later, cells were added with 2 μg/mL DiI-LDL (ADI Alpha Diagnostic International, San Antonio, USA) at 37 °C for 4 h. After cells were washed and resuspended with PBS, flow cytometer (ACEA NovoCyte, USA) was applied to measure the DiI fluorescence as described previously [32]. Additionally, DiI-LDL uptake by HepG2 cells treated as above was viewed by a Confocal Laser Scanning Microscope (FV500, Olympus, Tokyo, Japan).

4.3.6. ELISA assay

The serum PCSK9 levels in C57BL/6J mice were detected using the mouse PCSK9 simple step ELISA kit (Abcam). Briefly, all samples or standards were added to appropriate wells and subsequently the Antibody Cocktail was added. The plate was sealed and incubated for 1 h at room temperature on a plate shaker. Each well was washed with 3 × 350 μL 1× Wash Buffer PT. Then the TMB Development Solution was added and incubated for 20 min in the dark on a plate shaker. Finally, Stop Solution was added to each well and shaked plate on a plate shaker for 1 min to mix. The OD value at 450 nm was measured with a Victor X5 multilabel plate reader (PerkinElmer).

4.3.7. Statistical analyses

All Biological experiments were duplicated at least 3 independent times and the values were shown as the mean ± SEM. Student's *t*-test was applied to compare two groups and one-way ANOVA with Bonferroni's correction was used to compare the difference among multiple groups by GraphPad Prism Software. Two-sided *P*-values of <0.05 were considered a statistically significant difference.

Declaration of Competing Interest

The authors declare that they have no known competing financial interests or personal relationships that could have appeared to influence the work reported in this paper.

Acknowledgments

This work was supported by the CAMS initiative for innovative medicine (2019-I2M-1-005, 2016-I2M-2-002), the National Natural Science Foundation of China (81473214) and the Drug Innovation Major Project of China (2018ZX09711001-003-006).

Appendix A. Supplementary material

Supplementary data to this article can be found online at https://doi.org/10.1016/j.bioorg.2021.104994.

References

[1] G.A. Mensah, G.A. Roth, V. Fuster, The Global Burden of Cardiovascular Diseases and Risk Factors: 2020 and Beyond, J. Am. Coll. Cardiol. 74 (2019) 2529–2532.

[2] A.C. Burke, D.E. Telford, M.W. Huff, Bempedoic acid: effects on lipoprotein metabolism and atherosclerosis, Curr. Opin. Lipidol. 30 (2019) 1–9.

[3] Z.H. Tang, T.H. Li, J. Peng, J. Zheng, T.T. Li, L.S. Liu, Z.S. Jiang, X.L. Zheng, PCSK9: A novel inflammation modulator in atherosclerosis? J. Cell Physiol. 234 (2019) 2345–2355.

[4] M. Benn, B.G. Nordestgaard, P. Grande, P. Schnohr, A. Tybjaerg-Hansen, PCSK9 R46L, low-density lipoprotein cholesterol levels, and risk of ischemic heart disease: 3 independent studies and meta-analyses, J. Am. Coll. Cardiol. 55 (2010) 2833–2842.

[5] J. Cohen, A. Pertsemlidis, I.K. Kotowski, R. Graham, C.K. Garcia, H.H. Hobbs, Low LDL cholesterol in individuals of African descent resulting from frequent nonsense mutations in PCSK9, Nat. Genet. 37 (2005) 161–165.

[6] J.C. Cohen, E. Boerwinkle, T.H. Jr Mosley, H.H. Hobbs, Sequence variations in PCSK9, low LDL, and protection against coronary heart disease, N. Engl. J. Med. 354 (2006) 1264–1272.

[7] D.L. Dixon, L.G. Pamulapati, J.D. Bucheit, E.M. Sisson, S.R. Smith, C.J. Kim, G. F. Wohlford, J. Pozen, Recent updates on the use of PCSK9 inhibitors in patients with atherosclerotic cardiovascular disease, Curr. Atheroscler. Rep. 21 (2019) 16.

[8] D.J. Kereiakes, J.G. Robinson, C.P. Cannon, C. Lorenzato, R. Pordy, U. Chaudhari, H.M. Colhoun, Efficacy and safety of the proprotein convertase subtilisin/kexin type 9 inhibitor alirocumab among high cardiovascular risk patients on maximally tolerated statin therapy: The ODYSSEY COMBO I study, Am. Heart J. 169 (2015) 906–915.

[9] M.S. Sabatine, R.P. Giugliano, S.D. Wiviott, F.J. Raal, D.J. Blom, J. Robinson, C. M. Ballantyne, R. Somaratne, J. Legg, S.M. Wasserman, R. Scott, M.J. Koren, E. A. Stein, Efficacy and safety of evolocumab in reducing lipids and cardiovascular events, N. Engl. J. Med. 372 (2015) 1500–1509.

[10] F.J. Raal, E.A. Stein, R. Dufour, T. Turner, F. Civeira, L. Burgess, G. Langslet, R. Scott, A.G. Olsson, D. Sullivan, G.K. Hovingh, B. Cariou, I.G. Berthold, R. Somaratne, I. Bridges, R. Scott, S.M. Wasserman, D. Gaudet, PCSK9 inhibition with evolocumab (AMG 145) in heterozygous familial hypercholesterolaemia (RUTHERFORD-2): a randomised, double-blind, placebo-controlled trial, Lancet 385 (2015) 331–340.

[11] K.K. Ray, U. Landmesser, L.A. Leiter, D. Kallend, R. Dufour, M. Karakas, T. Hall, R. P. Troquay, T. Turner, F.L. Visseren, P. Wijngaard, R.S. Wright, J.J. Kastelein, Inclisiran in patients at high cardiovascular risk with elevated LDL cholesterol, N. Engl. J. Med. 376 (2017) 1430–1440.

[12] A.L. Catapano, A. Pirillo, G.D. Norata, New pharmacological approaches to target PCSK9, Curr. Atheroscler. Rep. 22 (2020) 24.

[13] D.S. Kazi, A.E. Moran, P.G. Coxson, J. Penko, D.A. Ollendorf, S.D. Pearson, J. A. Tice, D. Guzman, K. Bibbins-Domingo, Cost-effectiveness of PCSK9 inhibitor therapy in patients with heterozygous familial hypercholesterolemia or atherosclerotic cardiovascular disease, J. Am. Med. Assoc. 316 (2016) 743–753.

[14] S. Xu, S. Luo, Z. Zhu, J. Xu, Small molecules as inhibitors of PCSK9: Current status and future challenges, Eur. J. Med. Chem. 162 (2019) 212–233.

[15] P. Lo Surdo, M.J. Bottomley, A. Calzetta, E.C. Settembre, A. Cirillo, S. Pandit, Y. G. Ni, B. Hubbard, A. Sitlani, A. Carfí, Mechanistic implications for LDL receptor degradation from the PCSK9/LDLR structure at neutral pH, EMBO Rep. 12 (2011) 1300–1305.

[16] X.L. Wang, X.F. Chen, X.M. Zhang, C.Y. Su, M.X. Yang, W. He, Y. Du, S.Y. Si, L. Wang, B. Hong, A small-molecule inhibitor of PCSK9 transcription ameliorates atherosclerosis through the modulation of FoxO1/3 and HNF1α, EBioMedicine 52 (2020) 102650.

[17] J. Cameron, T. Ranheim, M.A. Kulseth, T.P. Leren, K.E. Berge, Berberine decreases PCSK9 expression in HepG2 cells, Atherosclerosis 201 (2008) 266–273.

[18] B. Dong, H. Li, A.B. Singh, A. Cao, J. Liu, Inhibition of PCSK9 transcription by berberine involves down-regulation of hepatic HNF1alpha protein expression through the ubiquitin-proteasome degradation pathway, J. Biol. Chem. 290 (2015) 4047–4058.

[19] H. Li, B. Dong, S.W. Park, H.S. Lee, W. Chen, J. Liu, Hepatocyte nuclear factor 1 alpha plays a critical role in PCSK9 gene transcription and regulation by the natural hypocholesterolemic compound berberine, J. Biol. Chem. 284 (2009) 28885–28895.

[20] S. Cao, P. Xu, J. Yan, H. Liu, L. Liu, L. Cheng, F. Qiu, N. Kang, Berberrubine and its analog, hydroxypropyl-berberrubine, regulate LDLR and PCSK9 expression via the ERK signal pathway to exert cholesterol-lowering effects in human hepatoma HepG2 cells, Cell Biochem. 120 (2018) 1340–1349.

[21] C.L. Wu, C. Xi, J.H. Tong, J. Zhao, H.L. Jiang, J. Wang, Y.P. Wang, H. Liu, Design, synthesis, and biological evaluation of novel tetrahydroprotoberberine derivatives (THPBs) as proprotein convertase subtilisin/kexin type 9 (PCSK9) modulators for the treatment of hyperlipidemia, Acta Pharm. Sin. B. 9 (2019) 1216–1230.

[22] W.J. Kong, J. Wei, P. Abidi, M.H. Lin, S. Inaba, C. Li, Y.L. Wang, Z.Z. Wang, S.Y. Si, H.N. Pan, S.K. Wang, J.D. Wu, Y. Wang, Z.R. Li, J.W. Liu, J.D. Jiang, Berberine is a novel cholesterol-lowering drug working through a unique mechanism distinct from statins, Nat. Med. 10 (2004) 1344–1351.

[23] Y.X. Wang, W.J. Kong, Y.H. Li, S. Tang, Z. Li, Y.B. Li, Y.Q. Shan, C.W. Bi, J.D. Jiang, D.Q. Song, Synthesis and structure–activity relationship of berberine analogues in LDLR up-regulation and AMPK activation, Bioorg. Med. Chem. 20 (2012) 6552–6558.

[24] Y.X. Wang, Y.P. Wang, H. Zhang, W.J. Kong, Y.H. Li, F. Liu, R.M. Gao, T. Liu, J. D. Jiang, D.Q. Song, Synthesis and biological evaluation of berberine analogues as novel up-regulators for both low-density-lipoprotein receptor and insulin receptor, Bioorg. Med. Chem. Let. 19 (2009) 6004–6008.

[25] T.Y. Fan, M.X. Ge, Z.H. Guo, H.W. He, N. Zhang, Y.H. Li, D.Q. Song, Discovery of 9O-substituted palmatine derivatives as a new class of anti-COL1A1 agents via repressing TGF-β1/Smads and JAK1/STAT3 pathways, Molecules 25 (2020) 773.

[26] T.Y. Fan, X.X. Guo, Q.X. Zeng, W. Wei, X.F. You, Y.X. Wang, J. Pang, D.Q. Song, Synthesis and structure-activity relationship of palmatine derivatives as a novel class of antibacterial agents against Helicobacter pylori, Molecules 25 (2020) 1352.

[27] T.Y. Fan, J. Pang, Q.X. Zeng, Y.X. Wang, X.F. You, D.Q. Song, Anti-Helicobacter pylori activities of 9-substituted palmatine derivatives, Acta Pharm. Sin. 55 (2020) 1237–1244.

[28] J. Chen, T. Wang, S. Xu, A. Lin, H. Yao, W. Xie, Z. Zhu, J. Xu, Design, synthesis and biological evaluation of novel nitric oxide-donating protoberberine derivatives as antitumor agents, Eur. J. Med. Chem. 132 (2017) 173–183.

[29] D.W. Zhang, T.A. Lagace, R. Garuti, Z.Z. Zhao, M. McDonald, J.D. Horton, J. C. Cohen, H.H. Hobbs, Binding of proprotein convertase subtilisin/kexin type 9 to epidermal growth factor-like repeat A of low density lipoprotein receptor decreases receptor recycling and increases degradation, J. Biol. Chem. 282 (2007) 18602–18612.

[30] N. Nassoury, D.A. Blasiole, A. Tebon Oler, N. Nassoury, D.A. Blasiole, A.T. Oler, S. Benjannet, J. Hamelin, V. Poupon, P.S. McPherson, A.D. Attie, A. Prat, N. G. Seidah, The cellular trafficking of the secretory proprotein convertase PCSK9 and its dependence on the LDLR, Traffic 8 (2007) 718–732.

[31] H. Li, B. Dong, S.W. Park, H.S. Lee, W. Chen, J.W. Liu, Hepatocyte nuclear factor 1α plays a critical role in PCSK9 gene transcription and regulation by the natural hypocholesterolemic compound Berberine, J. Biol. Chem. 284 (2009) 28885–28895.

[32] L. Wang, X.J. Jia, H.J. Jiang, Y. Du, F. Yang, S.Y. Si, B. Hong, MicroRNAs 185, 96, and 223 repress selective high-density lipoprotein cholesterol uptake through posttranscriptional inhibition, Mol. Cell. Biol. 33 (2013) 1956–1964.